

**Dieses Dokument ist eine Zweitveröffentlichung (Verlagsversion) /  
This is a self-archiving document (published version):**

Sebastian Zaunseder, Alexander Trumpp, Hannes Ernst, Michael Förster, Hagen Malberg

**Spatio-temporal analysis of blood perfusion by imaging  
photoplethysmography**

**Erstveröffentlichung in / First published in:**

*SPIE BiOS*. San Francisco, 2018. Bellingham: SPIE, Vol. 10501 {Zugriff am: 23.05.2019}.

DOI: <https://doi.org/10.1117/12.2289896>

Diese Version ist verfügbar / This version is available on:

<https://nbn-resolving.org/urn:nbn:de:bsz:14-qucosa2-351575>

„Dieser Beitrag ist mit Zustimmung des Rechteinhabers aufgrund einer (DFGgeförderten) Allianz- bzw. Nationallizenz frei zugänglich.“

This publication is openly accessible with the permission of the copyright owner. The permission is granted within a nationwide license, supported by the German Research Foundation (abbr. in German DFG).

[www.nationallizenzen.de/](http://www.nationallizenzen.de/)

# PROCEEDINGS OF SPIE

[SPIDigitalLibrary.org/conference-proceedings-of-spie](https://SPIDigitalLibrary.org/conference-proceedings-of-spie)

## Spatio-temporal analysis of blood perfusion by imaging photoplethysmography

Sebastian Zaunseder, Alexander Trumpp, Hannes Ernst, Michael Förster, Hagen Malberg

Sebastian Zaunseder, Alexander Trumpp, Hannes Ernst, Michael Förster, Hagen Malberg, "Spatio-temporal analysis of blood perfusion by imaging photoplethysmography," Proc. SPIE 10501, Optical Diagnostics and Sensing XVIII: Toward Point-of-Care Diagnostics, 105010X (20 February 2018); doi: 10.1117/12.2289896

**SPIE.**

Event: SPIE BiOS, 2018, San Francisco, California, United States

# Spatio-temporal analysis of blood perfusion by imaging photoplethysmography

Sebastian Zaunseder<sup>a</sup>, Alexander Trumpp<sup>a</sup>, Hannes Ernst<sup>a</sup>, Michael Förster<sup>a</sup>, and Hagen Malberg<sup>a</sup>

<sup>a</sup>TU Dresden, Institute of Biomedical Engineering, Fetscherstr. 29, 01307 Dresden, Germany

## ABSTRACT

Imaging photoplethysmography (iPPG) has attracted much attention over the last years. The vast majority of works focuses on methods to reliably extract the heart rate from videos. Only a few works addressed iPPGs ability to exploit spatio-temporal perfusion pattern to derive further diagnostic statements.

This work directs at the spatio-temporal analysis of blood perfusion from videos. We present a novel algorithm that bases on the two-dimensional representation of the blood pulsation (perfusion map). The basic idea behind the proposed algorithm consists of a pairwise estimation of time delays between photoplethysmographic signals of spatially separated regions. The probabilistic approach yields a parameter denoted as perfusion speed. We compare the perfusion speed versus two parameters, which assess the strength of blood pulsation (perfusion strength and signal to noise ratio).

Preliminary results using video data with different physiological stimuli (cold pressure test, cold face test) show that all measures are influenced by those stimuli (some of them with statistical certainty). The perfusion speed turned out to be more sensitive than the other measures in some cases. However, our results also show that the intraindividual stability and interindividual comparability of all used measures remain critical points.

This work proves the general feasibility of employing the perfusion speed as novel iPPG quantity. Future studies will address open points like the handling of ballistocardiographic effects and will try to deepen the understanding of the predominant physiological mechanisms and their relation to the algorithmic performance.

**Keywords:** Imaging photoplethysmography, remote sensing, camera, hemodynamics, perfusion

## 1. INTRODUCTION

Over the last years, the contact-less acquisition of cardiovascular parameters using cameras has gained immense attention. Similar to the clinically used photoplethysmography (PPG), the technique, referred to as imaging PPG (iPPG), camera-based PPG or remote PPG, exploits variations in light modulation due to the cardiovascular activity.

Most works in the field aim to extract the heart rate (e.g.<sup>1-3</sup>), heart rate variability (e.g.<sup>4-9</sup>) or respiratory rate (e.g.<sup>10</sup>). Some researchers even extracted the oxygen saturation (e.g.<sup>11-14</sup>) and information related to the morphology of iPPG signals (e.g.<sup>15</sup>). All such analyses base on the extraction of one-dimensional signals from a video stream by averaging the brightness over a region of interest (ROI). They thus resemble the conventional PPG.

Imaging photoplethysmography, however, provides two-dimensional information and thus allows spatio-temporal analyses of the blood perfusion via perfusion maps (the term *perfusion map* is used here to indicate a two-dimensional representation of blood pulsation that is gained from videos). Compared to laser doppler<sup>16,17</sup> or laser speckle,<sup>16,18</sup> which also yield two-dimensional information on the superficial perfusion, iPPG provides a simple and low-cost alternative. However, the theoretical fundamentals of suchlike analyses still have to be elaborated and up to date, only a few works have addressed two-dimensional analyses using iPPG.

---

Further author information: (Send correspondence to S.Z.)

S.Z.: E-mail: sebastian.zaunseder@tu-dresden.de, Telephone: +49 (0) 351 463 33786

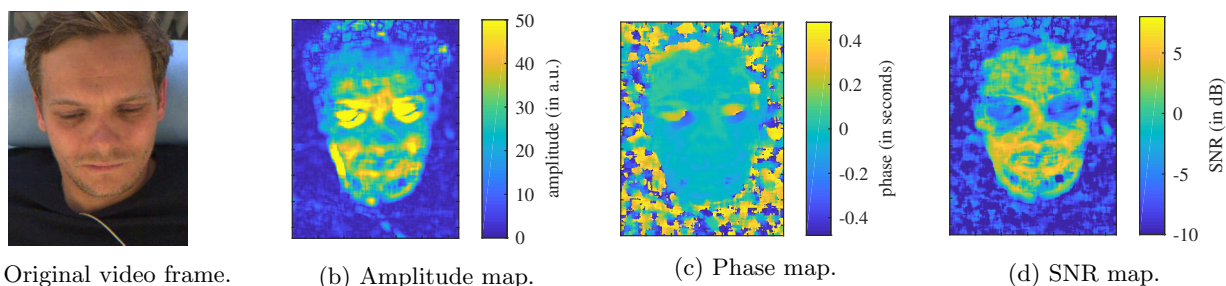


Figure 1: Exemplary perfusion maps generated based on the green channel. The procedure to obtain amplitude and phase maps is inspired by.<sup>19</sup> In our implementation we use two phase delayed sine waves whose frequency equals the heart rate as complex reference function. The SNR map was generated using the SNR definition by De Haan and Jeanne<sup>20</sup> (see also section 3.3). Note that high amplitudes in the amplitude map do not necessarily reflect usable signal but high energy artifacts can cause them.

This work presents a novel algorithm to assess the spatial blood perfusion from videos. We describe the algorithmic fundamentals of the proposed method and evaluate the method using experimental data involving different stimuli, namely cooling of a measurement site and application of a painful stressor. Our analysis directs at both, stability, i.e. how stable are the results of the proposed algorithm in a (quasi-)stationary state, and sensitivity, i.e. does the proposed method reveal changes caused by the stimuli.

The remainder of the article is structured as follows. In section 2 we will give a short overview on some existing approaches of spatial iPPG analyses and their limitations. Section 3 introduces the used data and details the proposed algorithm for spatial iPPG analysis. Section 4 and 5 present quantitative results on our data and discuss our findings concerning physiological and algorithmic aspects, respectively.

## 2. OVERVIEW ON APPROACHES FOR SPATIAL IPPG ANALYSES

Spatial iPPG analyses can be done in terms of the strength of blood pulsation or in terms of temporal differences of locally separated iPPG signals.

Different researchers have investigated spatial characteristics regarding the strength of blood pulsation. They make use of an absolute measure to quantify the strength of pulsation (e.g.<sup>14,15,19</sup>) or additionally normalize this measure to the noise component (e.g.<sup>21,22</sup>). Either way, they yield a two-dimensional representation of the blood pulsation (amplitude map). Corresponding analyses most often have a qualitative character, i.e. researchers primarily aimed to visualize static differences and used the resulting maps to define regions of interest (ROI) that are suited for other processing tasks (like extraction of the heart rate). Only a few works analyze the resulting maps in the context of (patho-)physiological changes. Zaproudina et al.<sup>23</sup> presented one analysis in this regard. They showed an altered symmetry of perfusion strength in case of migraine. Their investigation based on amplitude maps as proposed by Kamshilin et al.<sup>19</sup>

The alternative approach to exploit the spatial information directs at the temporal behavior of locally resolved iPPG signals. Several groups have assessed time differences between spatially separated regions thus yielding statements on the pulse transit time. To that end, synchronous recording of the palm and the face has been performed showing that varying time shifts can be detected by using cameras.<sup>24-26</sup> Even the time shift between nearby locations has been considered in so-called phase maps.<sup>27,28</sup> Frassinetti et al.<sup>29</sup> also evaluated the spatial behavior of temporal differences but the analysis strategy differed. They constructed a two-dimensional representation of blood pulsation\* by calculating time shifts of spatially separated iPPG signals to a reference function. The further analysis evaluated not a single time delay but the spatial distribution of the resulting phase map. The results show that the fractal behavior of such maps changes under influence of temperature variations.

Overall, the number of works that direct at spatial analyses is limited and two aspects seem to be particularly questionable.

\*The authors denote it as blood flow; however, according to the current understanding, it is a volume pulsation.

Firstly, different researchers found large time shifts within small regions (e.g. facial temporal differences of around  $-100$  ms to  $100$  ms in<sup>29</sup> (see also figure 1) or  $180$  degree phase shift at the wrist regions<sup>27</sup> were reported). One reason for such findings are different effects influencing the measurement signal, namely blood volume effects and ballistocardiographic effects.<sup>30,31</sup> The latter exhibit an arbitrary phase position. To avoid ballistocardiographic effects to impact the results, only homogeneous areas should be analyzed. However, the transition is fluent. Some areas, particularly all edges, are obviously affected by ballistocardiographic effects. But even in other supposedly homogeneous areas, subtle details like blood vessels can introduce heterogeneity and thus cause ballistocardiographic signal components, which can distort the analysis.

Secondly, at a macroscopic level, the "direction of blood supply" and pulse wave propagation, respectively, is not straightforward and nearby regions might be supplied by different arteries. Therefore, the relation between two explicit iPPG signals is not known. Using clearly separated regions, like the palm and the face, is a solution. However, the recording setup is impractical concerning real-life applications. It furthermore includes wide parts of the vasculature, which can hinder a proper interpretation of the findings. Within this contribution, we propose a novel algorithm, which tries to overcome such limitations and allows spatial iPPG analysis from locally restricted recordings.

### 3. METHODS AND MATERIALS

#### 3.1 Used data

The used data originates from two studies, namely a cold face test (CFT) study and a cold pressure test (CPT) study. Both experimental settings and information on the participants are detailed below.

**Cold face test study:** The study aimed at characterizing the capacity of cameras to capture physiological reactions caused by different stimuli, namely the application of a cold stressor and execution of a respiration maneuver. This contribution only focuses on the cold stress, which was applied by placing an ice pack (temperature  $< 0^{\circ}\text{C}$ ) on the forehead for 30s. Video data was recorded using four cameras operated at varying settings. The analysis of this contribution relies on a single RGB camera (UI-3370CP-C-HQ, IDS). The camera was configured with a color depth of 12 bit, a frame rate of 100 fps and an image resolution of  $420 \times 320$  pixels. Recordings were taken in the supine position at a distance of approximately 80 cm. The recording area typically covered the face and upper part of the thorax. The scenery was illuminated by ambient and a fluorescent ceiling light. As reference data, we recorded the non-invasive continuous blood pressure (Finometer Midi, Finapres Medical Systems), electrocardiogram, finger photoplethysmogram, and respiration by a thoracic belt (ADInstruments sensors). The captured data was synchronized via ADInstruments' PowerLab. The study was approved by the Institutional Review Board of the TU Dresden (EK168052013).

Figure 2 shows the experimental protocol. The data was analyzed in intervals of 10 s at specific time instants as indicated by figure 2. We defined three baseline intervals (*Baseline 1* - *Baseline 3*) to assess the stability of the used perfusion measures. The sensitivity of the perfusion measures was assessed by comparing intervals immediately before (*Before CFT1*-*Before CFT3*) and after (*After CFT1* - *After CFT3*) the application of the ice pack.

Overall 21 healthy subjects took part in the study (age  $26, 2 \pm 6, 69$  years, 6 female). Six recordings had to be discarded due to technical problems. All subjects gave written informed consent.

**Cold pressure test study:** The study aimed at characterizing the physiological reaction caused by a cold pressure test in dependency to the body positions (supine vs. sitting). The CPT is a widely used test that provokes a psychological and physiological reaction.<sup>32,33</sup> The cold pressure was applied by immersion of the hand into cold water (temperature  $3^{\circ}\text{C}$ ). The water temperature was controlled by a thermoregulator (TC45-F, Huber). The maximum time of immersion was three minutes. Subjects could terminate the immersion at each moment by removing their hand from the water. Video data was recorded using a single RGB camera (UI-3370CP-C-HQ, IDS). The camera was configured with a color depth of 12 bit, a frame rate 100 fps and an image resolution of  $420 \times 320$  pixels. Recordings were taken at a distance of approximately 80 cm (in both supine and sitting position). The recording area typically covered the face and upper part of the thorax. The scenery was illuminated by ambient and a fluorescent ceiling light. As reference data, we recorded the non-invasive continuous blood pressure (Finometer Midi, Finapres Medical Systems), electrocardiogram, finger photoplethysmogram, and

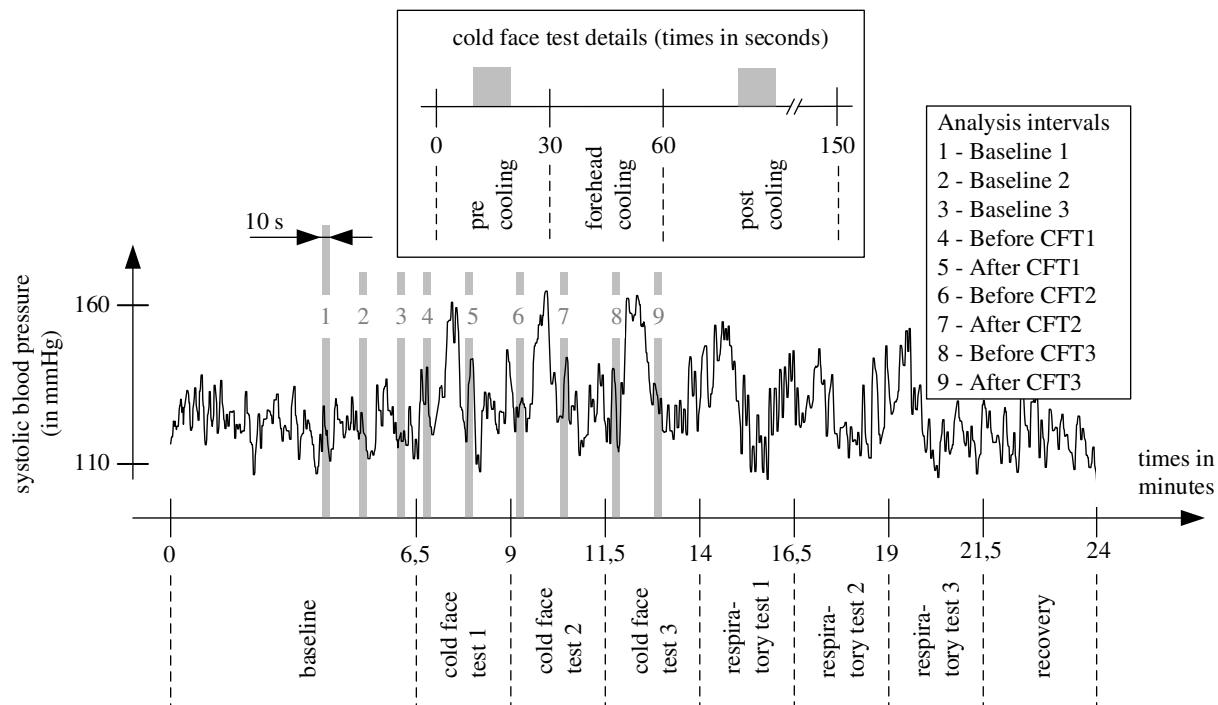


Figure 2: Experimental protocol of the cold face test study. Gray rectangles mark the analysis intervals (each interval has a length of 10s). Three baseline intervals (*Baseline 1*, *Baseline 2*, *Baseline 3*) are used to quantify the stability of the perfusion measures. The sensitivity of the perfusion measures is assessed by comparing intervals immediately before (*Before CFT1-Before CFT3*) and after (*After CFT1 - After CFT3*) the application of the ice pack. For this work the part related to the respiratory maneuvers has not been analyzed.

respiration by a thoracic belt (ADInstruments sensors). In addition, saliva samples were taken in order to analyze the cortisol and alpha-amylase levels, respectively. All data was synchronized via ADInstruments' PowerLab. The study was approved by the Institutional Review Board of the TU Dresden (EK119032016).

Figure 3 contains the experimental protocol. The data was analyzed in intervals of 10s at specific time instants as indicated by figure 3. We defined three baseline intervals (*Baseline 1*, *Baseline 2*, *Baseline 3*) to assess the stability of the perfusion measures. The sensitivity of the perfusion measures was primarily assessed by comparing *Baseline 3* vs. *Highest SBP* (time instant that showed the highest systolic blood pressure). *Start CPT* defines the time interval 10s after immersion of the hand into cold water which serves as illustration for the immediate response to the test.

Overall 22 healthy subjects took part in the study (age 25,  $5 \pm 3.73$  years, 10 female). All subjects executed the test twice on different days, one time in supine and one time in sitting position. Due to the varying recording positions and temporally separated recordings, the single recordings were considered independent for the statistical analysis. One recording had to be discarded due to technical problems resulting in 43 usable data sets<sup>†</sup>. All subjects gave written informed consent.

### 3.2 Basic concept to assess the perfusion

The basic idea behind the proposed method is the pairwise estimation of time delays between iPPG signals of locally separated regions. For the iPPG signal of a point  $P_0$ , we derive the time delays  $\Delta t_{P_n}^{P_0}$  to the iPPG signals of the surrounding points  $P_n$  with  $n$  referring to any other point. The division of  $\Delta t_{P_n}^{P_0}$  by the distance  $d_0^n$  between  $P_0$  and  $P_n$  yields a velocity distribution  $V^{P_0}$  for point  $P_0$ . This distribution can be understood as a

<sup>†</sup>Note that additional recordings were excluded by further processing steps mainly due to subjects' movements. For more details, see section 3.3.

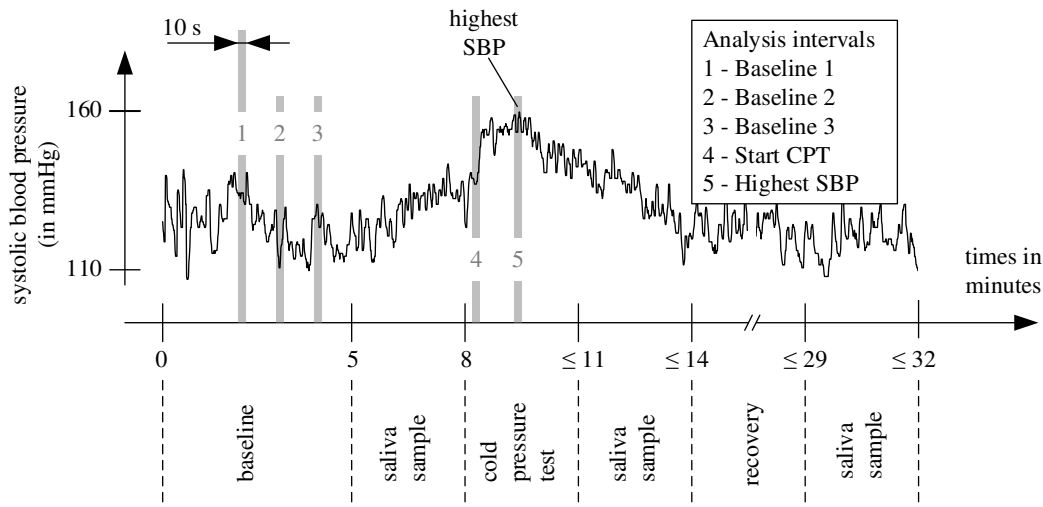


Figure 3: Experimental protocol of the cold pressure test. Gray rectangles mark the used analysis intervals (each interval has a length of 10 s). Three baseline intervals (*Baseline 1*, *Baseline 2*, *Baseline 3*) were used to quantify the stability of the perfusion measures. The sensitivity of the perfusion measure was primarily assessed by comparing *Baseline 3* vs. *Highest SBP* (time instant which showed the highest systolic blood pressure). *Start CPT* defines the time interval 10 s after immersion of the hand into cold water which serves as illustration for the immediate response to the test.

probabilistic estimate of the pulse wave propagation speed belonging to  $P_0$ . The process is applied to all points  $P$  thus yielding a set of distribution  $V^P$ . From their combination, we derive an estimate for the pulse wave propagation speed, which we denote as perfusion speed. Figure 4 illustrates the procedure for an exemplary point.

Note that the proposed measure nor is a speed in a strict sense (see also section 3.3), neither it should be treated as equivalent to the conventional pulse wave velocity. However, it is intended to characterize the propagation of pulse wave and the underlying algorithm relates to the calculation of a speed. The term *perfusion speed* reflects both aspects.

### 3.3 Implementation

The proposed algorithm provides a framework with several degrees of freedom. In the following paragraph, the details of our current implementation are presented. It should be noted that the focus of this work is to prove the feasibility and provide a first characterization of the novel algorithm. Although a fully automated implementation relying solely on camera data is feasible, the presented implementation incorporates reference data, namely heart rate estimations from the reference ECG, and some manual annotations, namely the definition of an ROI on the forehead. Either step could be done based on the video data. However, erroneous heart rate detections or ROI definitions, respectively, will tamper the algorithmic performance and make interpretation more difficult. We, therefore, decided against a fully automated version.

**Spatial restrictions:** We apply the proposed algorithm to a manually defined ROI centered on the forehead (i.e. the points  $P$  all lie inside the ROI). By restricting the processing to the forehead, the influence of ballistocardiographic effects should be reduced<sup>15,30</sup> and we avoid erroneous segmentation to interfere with the algorithmic performance.

**Preprocessing:** We transformed the videos from the RGB to the HSI color space and used the hue channel because this channel was shown to efficiently capture the blood pulsation.<sup>34,35</sup> We further spatially smoothed the input images by a moving average filter of the size  $15 \times 15$  pixels (in previous tests this size turned out to be suited to suppress noise and yield a high signal-to-noise ratio (SNR) for the used cameras). The time varying signals from the smoothed images served as input iPPG signals to the algorithm. All iPPG signals were bandpass

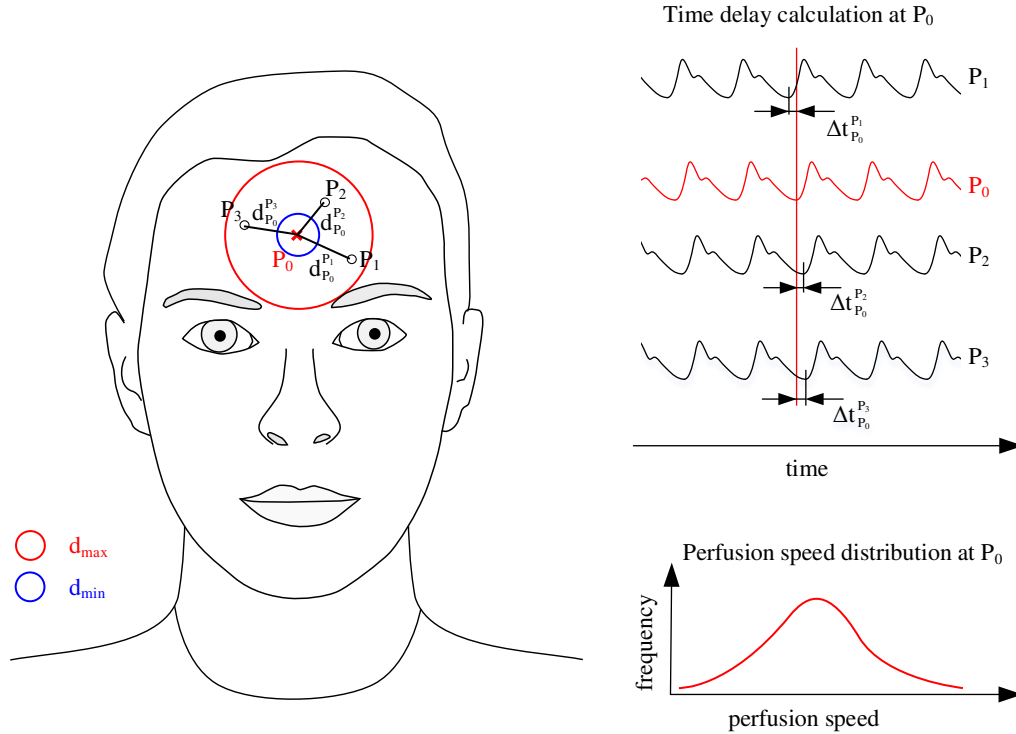


Figure 4: Basic principle underlying the proposed algorithm to assess the pulse wave propagation. For a point  $P_0$  time delays to  $P_n$  are calculated to estimate a velocity distribution.  $d_{max}$  and  $d_{min}$  are optional to limit the distance in which the pairwise comparisons are done.

filtered by an IIR filter (5th order butterworth filter; lower cutoff frequency 0.5 Hz, upper cutoff frequency 6 Hz). Finally, iPPG signals that showed a SNR lower than  $-8$  dB were excluded from further processing. The used SNR definition follows the ideas of de Haan and Jeanne.<sup>20</sup> It regards the power of the heart rate  $f_{hr} \pm 5$  bpm and the first harmonic  $f_{hr1} \pm 5$  bpm as wanted signal. The noise component was calculated by the residual power within  $[\lambda_1, \lambda_2]$  with  $\lambda_1 = 30$  bpm and  $\lambda_2 = 240$  bpm. The SNR (in dB) is defined as

$$SNR = 10 \log_{10} \left( \frac{\sum_{k=\lambda_1}^{\lambda_2} \Pi(k) |X(k)|^2}{\sum_{k=\lambda_1}^{\lambda_2} (1 - \Pi(k)) |X(k)|^2} \right) \quad (1)$$

where the binary mask  $\Pi$  reads to

$$\Pi(k) = \begin{cases} 1, & \text{if } |f_{hr} - \Delta f \cdot k| \leq 5 \text{ bpm} \\ 1, & \text{if } |f_{hr1} - \Delta f \cdot k| \leq 5 \text{ bpm} \\ 0, & \text{otherwise} \end{cases} \quad (2)$$

The heart rate  $f_{hr}$  is taken from the reference ECG.

**Estimation of time delays:** To estimate the time delays between spatially separated iPPG signals, we used the phase information of our 10 s segments. Similar to the method proposed by Kamshilin et al.,<sup>19</sup> we multiplied the pixel traces by a complex reference function. In our case, two phase delayed sine waves with the frequency of  $f_{hr}$  (again taken from the reference ECG) served as reference function. The multiplication yields a complex perfusion map. From this map, we calculated the phase, i.e. the spatially resolved information on the signal phase (see figure 1).

**Calculation of point distances:** To calculate the distance between considered points we determined the

Euclidean distance between  $P_0$  and  $P_n$  according to

$$d_{P_0}^{P_n} = \sqrt{(x_{P_0} - x_{P_n})^2 + (y_{P_0} - y_{P_n})^2} \quad (3)$$

where  $x$  and  $y$  are the coordinates of the considered points in pixels. To construct the histograms, we only considered pairs of points that have a distance  $20 > d > 70$  (i.e.  $d_{min} = 20$  and  $d_{max} = 70$ ). Note that using the Euclidean distance is intuitive but arbitrary. Due to the calculation in pixels we neither yield a physical speed nor can transfer these numbers to other data. However, as our recording conditions were similar in both studies, we used the same definition and distances in pixels.

**Histogram processing:** According to section 3.2, the proposed method yields a set of histograms from which the perfusion speed is estimated. In the current implementation, histograms are generally constructed using 200 bins. For all histograms, the lower boundary is defined as  $2/3$  of the 5. percentile of all calculated velocities (i.e. the velocities between all points). The upper boundary is the 80th percentile.

### 3.4 Alternative measures to assess the perfusion

In order to comparatively evaluate the proposed method, we implemented two other measures to assess the perfusion. Firstly, we calculated the strength of pulsation (further denoted as perfusion strength). Similar to the way to determine the phase information, even the perfusion strength bases on the multiplication of local iPPG signals by a complex reference function according to.<sup>19</sup> As before, the multiplication yields a complex perfusion map. We calculate the perfusion strength as the mean of the absolute values of the perfusion map within the ROI. To calculate the perfusion strength, the green channel was used because the normalization within the transformation to HSI might suppress changes in pulsation strength. Further, light within the green wavelength range was previously shown to indicate changes in perfusion.<sup>15,23,36,37</sup>

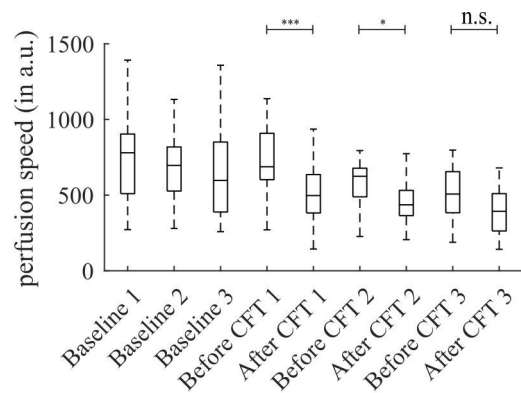
Besides the perfusion strength, we use the SNR as described in section 3.3 to assess changes in the perfusion. Again, we calculate the SNR of the local iPPG signals and we take the mean over the ROI to yield a single measure to access the perfusion. The SNR was calculated for both, the hue channel and the green channel.

Both measures, perfusion strength and SNR, are applied to spatially smoothed video data with the same ROIs as used for the perfusion speed in order to make these measures comparable to the perfusion speed. Regarding the perfusion strength, we also discarded iPPG signals that showed an SNR lower than  $-8$  dB.

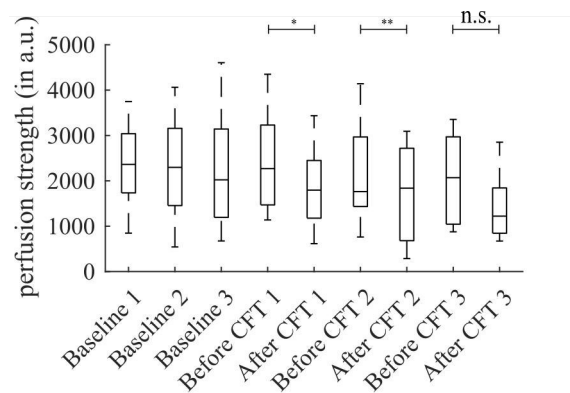
### 3.5 Exclusion criteria and statistical assessment

Particularly the CPT introduces persistent displacements of the subjects' heads during or after putting the hand into the water reservoir. Strong displacements hinder that the same areas on the forehead can be identified and be used as ROIs. An altered ROI is likely to impact the results and makes their interpretation difficult. We, therefore, excluded all subjects who showed a high ROI variation in at least one of the considered analysis intervals. The variation is measured by using the two-dimensional correlation coefficient between ROI masks of different analysis intervals (the ROI mask is a binary mask with logical 1 for pixels of the ROI). If the correlations between at least one pair of ROI masks in a subject is lower than 0.6, the recording was considered as not suitable and the respective subject was excluded from statistical analysis.

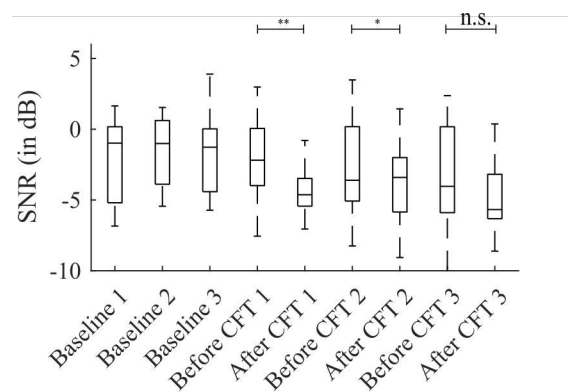
To assess the used perfusion measures statistically, we compared the analysis intervals from each experiment by using a Friedman test (range based test for paired data). As post-hoc tests, we applied the Wilcoxon test. Post-hoc tests are carried out only between analysis intervals where we assumed differences, i.e. between an interval in which we expect a physiological reaction and its closest baseline interval. Accordingly, we compared *Baseline 3* versus *Start CPT* and *Highest SBP*, respectively, for the CPT study. For the CFT study, we compared *Before CFT1* versus *After CFT1*, *Before CFT2* versus *After CFT2* and *Before CFT3* versus *After CFT3*). As we did not expect differences between baseline intervals, we did not apply post-hoc tests to such intervals, but we only considered their descriptive statistics to estimate the stability of the used perfusion measures.



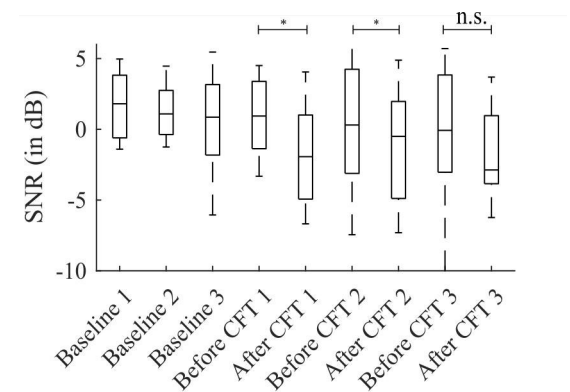
(a) Perfusion speed (based on the hue channel). Friedman test showed very highly significant differences ( $p < 0.001$ ).



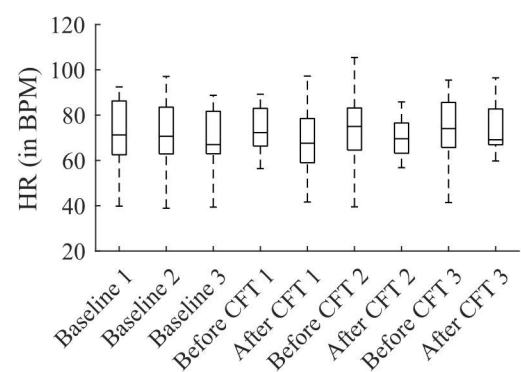
(b) Perfusion strength (based on the green channel). Friedman test showed highly significant differences ( $p < 0.01$ ).



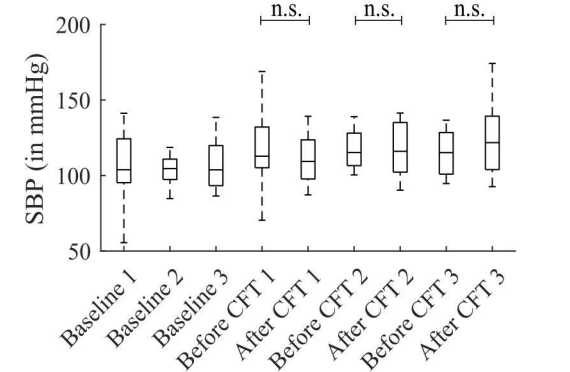
(c) SNR of hue channel. Friedman test showed very highly significant differences ( $p < 0.001$ ).



(d) SNR of green channel. Friedman test showed very highly significant differences ( $p < 0.001$ ).

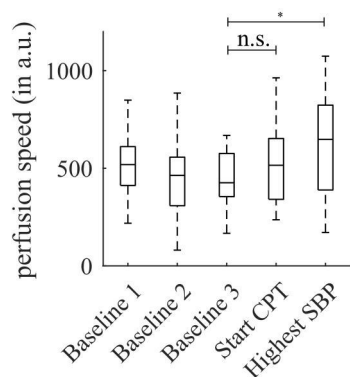


(e) Heart rate. Friedman test showed no significant difference.

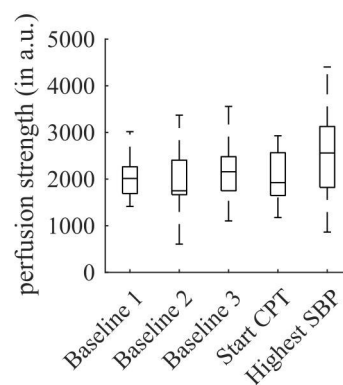


(f) Systolic blood pressure. Friedman test showed very highly significant differences ( $p < 0.001$ ).

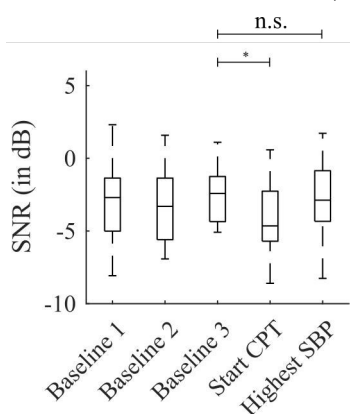
Figure 5: Results of the CFT study (outliers are not shown). Horizontal bars indicate combinations to which post-hoc testing applied (precondition to post-hoc testing is a significant Friedman test). The results of the post-hoc tests are also shown (n.s. –  $p \geq 0.05$ , \* –  $p < 0.05$ , \*\* –  $p < 0.01$ , \*\*\* –  $p < 0.001$ ). It should be noted that the large spread is (partially) caused by interindividual differences. Statistical testing considers paired data.



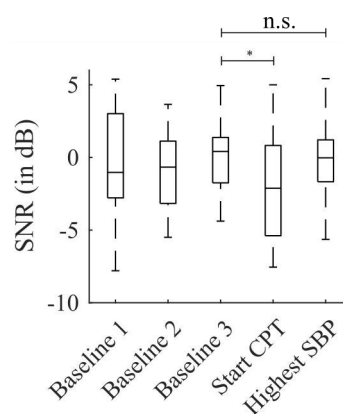
(a) Perfusion speed (based on the hue channel). Friedman test showed significant differences ( $p < 0.05$ ).



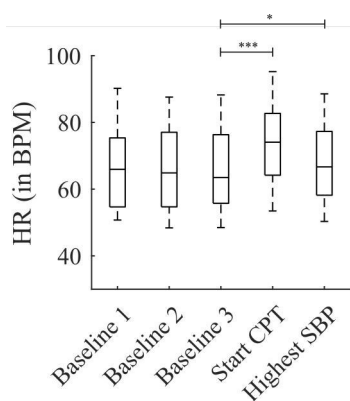
(b) Perfusion strength (based on the green channel). Friedman test showed no significant difference.



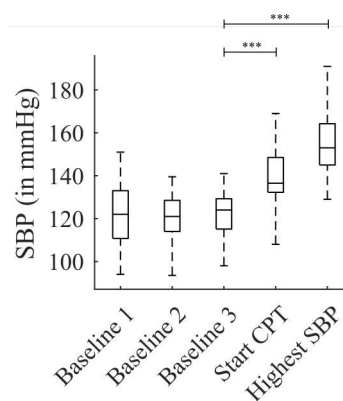
(c) SNR of hue channel. Friedman test showed significant differences ( $p < 0.05$ ).



(d) SNR of green channel. Friedman test showed significant differences ( $p < 0.05$ ).



(e) Heart rate. Friedman test showed very highly significant differences ( $p < 0.001$ ).



(f) Systolic blood pressure. Friedman test showed very highly significant differences ( $p < 0.001$ ).

Figure 6: Results of the CPT study (outliers are not shown). Horizontal bars indicate combinations to which post-hoc testing applied (precondition to post-hoc testing is a significant Friedman test). The results of the post-hoc tests are also shown (n.s. –  $p \geq 0.05$ , \* –  $p < 0.05$ , \*\* –  $p < 0.01$ , \*\*\* –  $p < 0.001$ ). It should be noted that the large spread is (partially) caused by interindividual differences. Statistical testing considers paired data.

## 4. RESULTS

Figure 5 and figure 6 show the results of the CFT study and CPT study, respectively. The exclusion criteria from section 3.5 discarded 22 recordings of the CPT study (the analysis thus bases on 21 of 43 recordings). For the CFT study, no recordings were discarded based on the aforementioned criterion on the ROI.

Both studies show significant differences for the perfusion speed as indicated by the Friedman test (CPT study  $p = 0.019$ , CFT study  $p \approx 0$ ). For the CFT study, the post-hoc tests reveal a significant difference for the first and second application of the cold stressor. For the CPT study, the post-hoc tests reveal a significant difference between *Baseline 3* and *Highest SBP* (15 of 21 subjects show an increased perfusion speed) but not between *Baseline 3* and *Start CPT* (here a trend can be observed).

For the CFT study, even the perfusion strength and SNR (hue channel and green channel) show significant differences. For the CPT study, the Friedman test does not show significant differences for the perfusion strength but only for the SNR (with a reduction at *Start CPT* compared to *Baseline 3* for the hue and green channel).

The analysis of baseline intervals reveals a considerable spread under (quasi-)stationary conditions. For both studies, this spread is less pronounced than the changes introduced by the stimuli, but it covers a similar range.

## 5. DISCUSSION

### 5.1 Interpretation of the results

At first glance, the results of the CFT study are surprising because cooling is generally associated with vasoconstriction. During vasoconstriction, one could expect an increased perfusion speed but according to figure 5 the perfusion speed decreases. One explanation is the time of analysis. As the analysis interval had to be placed after the removal of the ice pack, it is likely that the process of recovery already started (recovery concerning global hemodynamics and local perfusion; the first can be seen by the systolic blood pressure). Another explanation might be local regulatory effects. According to Drummond, injury or painful stimulation of the facial skin can initiate local vasodilation.<sup>38</sup> Both facts can explain a decrease in the perfusion speed. However, perfusion strength and SNR also show a marked decrease after the application of the cold stimuli. Although there might be other explanations, we associate a decrease in such measures either to a reduced pulse pressure<sup>39</sup> or to a local vasoconstriction. According to our reference data, the pulse pressure remains stable, which accounts for vasoconstriction being present. Accordingly, the behavior of the pulse strength and SNR are contradictory to the perfusion speed. A possible explanation might be an undesired interaction with the SNR which also has a very characteristic behaviour. The SNR decreases significantly to a level at which more pixels will be excluded from the further analysis (see  $-8$  dB threshold). However, in the CPT study, we also observed a markedly decreased SNR at the interval *Start CPT* (see figure 6). In this case, the perfusion speed does not decrease, but it slightly increases. This observation might indicate that the SNR is at least not solely responsible for our observation. Nevertheless, future investigations will have to clarify the role of the SNR. Another explanation might be an increased heterogeneity of the perfusion as a result of vasoconstriction. In the context of skin cooling, Frassinetti et al.<sup>29</sup> revealed a more heterogeneous pattern in defined perfusion maps (time shifts). However, even heterogeneity does not right away provide an explanation to the observed behaviour, but it could be a starting point so that even this theory has to be carefully revised in the future.

Compared to the CFT study, the results of the CPT study can be well explained. The highest systolic blood pressure leads to the largest change in the perfusion speed and perfusion strength (the latter not being significant). Concerning the perfusion speed, in *Start CPT*, an increase is already visible but not pronounced. The SNR for both, the hue channel and the green channel, show a decrease after the start of the CPT. This reduction might be the result of vasoconstriction or slight movements within the analysis intervals.

All results show high intraindividual and interindividual variations. Intraindividual variations must be attributed to the algorithms underlying the used measures. Minor physiological changes (as they are expected even at rest) or factors like subtle movements and displacements, respectively, introduce large variations in the used measures. This behaviour limits the applicability of all measures in their current form. Thus, future works should address the stability of perfusion measures. Interindividual variations reflect the deviating anatomy and physiology of the participants. E.g. for the CPT, individual differences in the physiological reaction have been

described.<sup>40</sup> This individuality expresses in an even higher variance at *Highest SBP* compared to the baseline intervals.

So far, we did not perform a direct comparison of the perfusion speed to other approaches that exploit temporal differences in locally separated iPPG signals. A suchlike comparison is difficult because previous approaches typically require the definition of areas to be used. It is likely that the results of any comparison will heavily depend on the chosen areas. However, both approaches have a common ground, namely the general idea to exploit temporal differences from iPPG signals. In our understanding, the proposed method offers two advantages: (i) it relaxes the assumptions on the direction of pulse wave propagation, and (ii) it should be more stable due to the probabilistic integration of much more information. However, care should be taken when comparing our method to approaches that use separated areas like the face and the palm. Suchlike analyses might not be comparable because the latter approach integrates more global effects whereas our method is expected to yield more local information.

## 5.2 Further experiments

During the development of the proposed method, we carried out different experiments which were not shown in this contribution. Such experiments included the usage of alternative ROIs. On the one hand, we applied the used measures to the presented data but used the whole face, i.e. did not restrict the analyses to the forehead area. On the other hand, we used other data, namely video recordings of the inner forearm and the back of the hand during warming. In both cases, ballistocardiographic effects were troublesome because the alternative measurement sides and ROIs, respectively, show stronger inhomogeneities. Moreover, when recording the extremity, the utilization of the SNR becomes very critical. Compared to the face, the forearm and the back of hand, respectively, show a markedly decreased signal quality (see e.g.<sup>41,42</sup>). Although averaging yields a usable signal, the low signal quality hampers spatial analyses that must operate with limited averaging sizes or even without averaging at all. Future works will focus on preprocessing methods to increase the SNR and automatically suppress ballistocardiographic effects. Particularly in case of low SNR, the inclusion of source separation techniques might be beneficial.<sup>43</sup> In combination with advanced methods to identify usable skin regions based on their homogeneity,<sup>31</sup> the spatial analysis might become possible in areas other than the forehead.

## 5.3 Limitations

We could show that the used measures can reveal differences caused by applied stimuli. In this regard, the perfusion speed turned out to be sometimes even more sensitive than alternative measures with respect to the applied stimuli.

However, the required exclusion of recordings means a major limitation concerning the real world applicability of the proposed method. As stated before, the presented work is restricted to the analysis of feasibility. Against that background, our restriction to recordings with stable ROIs can be justified. The real-world usage, however, requires a method to cope with varying ROIs, which is currently not the case.

The degrees of freedom of the proposed method imply another limitation. The current form represents one possible realization of the basic algorithmic concept. Other parameter combinations will lead to altered results, and future works should investigate the impact of the algorithmic parameterization. Moreover, the usage of phase information to estimate the time delay generally has disadvantages because the phase is derived from signals of 10 s. Using signal segments introduces a temporal blurring. Furthermore, due to the current phase calculation by multiplication with a reference function at a fixed frequency, the heart rate variability might introduce undesired effects. Future works will, therefore, consider the beat-to-beat extraction of time delays in the time domain as alternative to the usage of phase information.

Last and most importantly, a more detailed characterization of the physiological changes upon the applied stimuli and its effect on the algorithmic behaviour is pending. In the face of the complex interactions between global and local hemodynamic effects and interindividual differences, the analysis of mean results by statistical methods, as presented here, is not enough. Future works must conduct a detailed analysis on an individual level in order to better understand the algorithmic performance.

## 6. CONCLUSIONS

In this paper, we presented a novel algorithm to capture the spatial perfusion from videos. As stated before, more analyses are necessary to characterize the proposed method more deeply. However, independently of the exact physiological and technical determinants, which lead to our results, the proposed algorithm turned out to be more sensitive to external stimuli than other camera-based measures. This finding motivates further investigations on the topic.

## ACKNOWLEDGMENTS

This work was funded by the "Bundesministerium für Bildung und Forschung" (BMBF) (project "fast care - Kamerabasiertes Monitoring", ref. 03ZZ0519C).

We thank all volunteers for their participation. We further thank Ms. Anna Stumpf and Mr. Peter Lochmann for their contribution within the process of data collection.

## REFERENCES

- [1] Poh, M.-Z., McDuff, D. J., and Picard, R. W., "Non-contact, automated cardiac pulse measurements using video imaging and blind source separation," *Opt. Express* **18**, 10762–74 (2010).
- [2] Rasche, S., Trumpp, A., Waldow, T., Gaetjen, F., Plötze, K., Wedekind, D., Schmidt, M., Malberg, H., Matschke, K., and Zaunseder, S., "Camera-based photoplethysmography in critical care patients," *Clin. Hemorheol. Microcirc.* **64**, 77–90 (2016).
- [3] Wang, W., Stuijk, S., and de Haan, G., "Exploiting Spatial Redundancy of Image Sensor for Motion Robust rPPG," *IEEE Trans. Biomed. Eng.* **62**(2), 415–25 (2015).
- [4] Iozzia, L., Cerina, L., and Mainardi, L., "Relationships between heart-rate variability and pulse-rate variability obtained from video-PPG signal using ZCA," *Physiol. Meas.* **37**, 1934–1944 (2016).
- [5] McDuff, D., Gontarek, S., and Picard, R. W., "Improvements in Remote Cardiopulmonary Measurement Using a Five Band Digital Camera," *IEEE Trans. Biomed. Eng.* **61**, 2593–2601 (2014).
- [6] Moreno, J., Ramos-Castro, J., Movellan, J., Parrado, E., Rodas, G., and Capdevila, L., "Facial Video-Based Photoplethysmography to Detect HRV at Rest," *Int. J. Sports Med.* **36**, 474–480 (2015).
- [7] Poh, M.-Z., McDuff, D. J., and Picard, R. W., "Advancements in noncontact, multiparameter physiological measurements using a webcam," *IEEE Trans. Biomed. Eng.* **58**, 7–11 (2011).
- [8] Liang, C., Li, Y., and Luo, J., "A Novel Method to Detect Functional microRNA Regulatory Modules by Bicliques Merging," in [*IEEE/ACM Trans. Comput. Biol. Bioinforma.*], **13**(3), 549–56 (2017).
- [9] Zaunseder, S., Heinke, A., Trumpp, A., and Malberg, H., "Heart beat detection and analysis from videos," in [*2014 IEEE 34th Int. Sci. Conf. Electron. Nanotechnol.*], 286–290, IEEE (2014).
- [10] Zhao, F., Li, M., Qian, Y., and Tsien, J. Z., "Remote measurements of heart and respiration rates for telemedicine," *PLoS One* **8**(10), e71384 (2013).
- [11] Bal, U., "Non-contact estimation of heart rate and oxygen saturation using ambient light," *Biomed. Opt. Express* **6**, 86–97 (2015).
- [12] Guazzi, A. R., Villarroel, M., Jorge, J., Daly, J., Frise, M. C., Robbins, P. a., and Tarassenko, L., "Non-contact measurement of oxygen saturation with an RGB camera," *Biomed. Opt. Express* **6**, 3320 (2015).
- [13] Kong, L., Zhao, Y., Dong, L., Jian, Y., Jin, X., Li, B., Feng, Y., Liu, M., Liu, X., and Wu, H., "Non-contact detection of oxygen saturation based on visible light imaging device using ambient light," *Opt. Express* **21**, 17464 (2013).
- [14] Tarassenko, L., Villarroel, M., Guazzi, A., Jorge, J., Clifton, D. a., and Pugh, C., "Non-contact video-based vital sign monitoring using ambient light and auto-regressive models," *Physiol. Meas.* **35**, 807–31 (2014).
- [15] Trumpp, A., Schell, J., Malberg, H., and Zaunseder, S., "Vasomotor assessment by camera-based photoplethysmography," *Curr. Dir. Biomed. Eng.* **2**, 199–202 (2016).
- [16] Briers, J. D., "Laser Doppler, speckle and related techniques for blood perfusion mapping and imaging," *Physiol. Meas.* **22**, R35–66 (2001).

- [17] Leahy, M. J., de Mul, F. F., Nilsson, G. E., and Maniewski, R., "Principles and practice of the laser-Doppler perfusion technique," *Technol. Health Care* **7**(2-3), 143–62 (1999).
- [18] Draijer, M., Hondebrink, E., Van Leeuwen, T., and Steenbergen, W., "Review of laser speckle contrast techniques for visualizing tissue perfusion," *Lasers Med. Sci.* **24**(4), 639–651 (2009).
- [19] Kamshilin, A. A., Miridonov, S., Teplov, V., Saarenheimo, R., and Nippolainen, E., "Photoplethysmographic imaging of high spatial resolution," *Biomed. Opt. Express* **2**, 996–1006 (2011).
- [20] de Haan, G. and Jeanne, V., "Robust pulse rate from chrominance-based rPPG," *IEEE Trans. Biomed. Eng.* **60**, 2878–86 (2013).
- [21] Fallet, S., Moser, V., Braun, F., and Vesin, J.-M., "Imaging Photoplethysmography: What are the Best Locations on the Face to Estimate Heart Rate?," in [*Comput. Cardiol. (2010)*], 341–344 (2016).
- [22] Lempe, G., Zaunseder, S., Wirthgen, T., Zipser, S., and Malberg, H., "ROI Selection for Remote Photoplethysmography," in [*Bild. für die Medizin 2013*], Meinzer, H.-P., Deserno, T. M., Handels, H., and Tolxdorff, T., eds., 99–103, Springer, Heidelberg (2013).
- [23] Zaproudina, N., Teplov, V., Nippolainen, E., Lipponen, J. a., Kamshilin, A. a., Närhi, M., Karjalainen, P. a., and Giniatullin, R., "Asynchronicity of facial blood perfusion in migraine," *PLoS One* **8**, e80189 (2013).
- [24] Jeong, I. C. and Finkelstein, J., "Introducing Contactless Blood Pressure Assessment Using a High Speed Video Camera," *J. Med. Syst.* **40**, 77 (2016).
- [25] Shao, D., Yang, Y., Liu, C., Tsow, F., Yu, H., and Tao, N., "Noncontact monitoring breathing pattern, exhalation flow rate and pulse transit time," *IEEE Trans. Biomed. Eng.* **61**, 2760–7 (2014).
- [26] Secerbegovic, A., Bergsland, J., Halvorsen, P. S., Suljanovic, N., Mujcic, A., and Balsasingham, I., "Blood Pressure Estimation Using Video Photoplethysmography," in [*13th Int. Symp. Biomed. Imaging*], 461–464 (2016).
- [27] Kamshilin, A. A., Nippolainen, E., Sidorov, I. S., Vasilev, P. V., Erofeev, N. P., Podolian, N. P., and Romashko, R. V., "A new look at the essence of the imaging photoplethysmography," *Sci. Rep.* **5**, 10494 (2015).
- [28] Yang, J., Guthier, B., and Saddik, A. E., "Estimating two-dimensional blood flow velocities from videos," in [*2015 IEEE Int. Conf. Image Process.*], 3768–3772, IEEE (2015).
- [29] Frassinetti, L., Giardini, F., Perrella, A., Sorelli, M., Sacconi, L., and Bocchi, L., "Evaluation of spatial distribution of skin blood flow using optical imaging," in [*C. 2017 Proc. Int. Conf. Med. Biol. Eng. 2017*], 74–80 (2017).
- [30] Moco, A. V., Stuijk, S., and de Haan, G., "Ballistocardiographic Artifacts in PPG Imaging," *IEEE Trans. Biomed. Eng.* **63**, 1804–11 (2016).
- [31] Trumpp, A., Rasche, S., Wedekind, D., Schmidt, M., Waldow, T., Gaetjen, F., Plötze, K., Malberg, H., Matschke, K., and Zaunseder, S., "Skin Detection and Tracking for Camera-Based Photoplethysmography Using a Bayesian Classifier and Level Set Segmentation," in [*Bild. für die Medizin 2017*], 43–48 (2017).
- [32] Lovullo, W., "The cold pressor test and autonomic function: a review and integration," *Psychophysiology* **12**, 268–82 (1975).
- [33] Skoluda, N., Strahler, J., Schlotz, W., Niederberger, L., Marques, S., Fischer, S., Thoma, M. V., Spoerri, C., Ehlert, U., and Nater, U. M., "Intra-individual psychological and physiological responses to acute laboratory stressors of different intensity," *Psychoneuroendocrinology* **51**, 227–36 (2015).
- [34] Lueangwattana, C., Kondo, T., and Haneishi, H., "A Comparative Study of Video Signals for Non- contact Heart Rate Measurement," in [*12th Int. Conf. Electr. Eng. Comput. Telecommun. Inf. Technol.*], 1–5 (2015).
- [35] Tsouri, G. R. and Li, Z., "On the benefits of alternative color spaces for noncontact heart rate measurements using standard red-green-blue cameras," *J. Biomed. Opt.* **20**(4), 048002 (2015).
- [36] Kamshilin, A. A., Teplov, V., Nippolainen, E., Miridonov, S., and Giniatullin, R., "Variability of microcirculation detected by blood pulsation imaging," *PLoS One* **8**, e57117 (2013).
- [37] Rubins, U., Miscuks, A., and Lange, M., "Simple and convenient remote photoplethysmography system for monitoring regional anesthesia effectiveness," in [*IFMBE Proc.*], 378–381 (2018).
- [38] Drummond, P. D., "Psychophysiology of the blush," in [*Psychol. Significance Blush*], Crozier, W. R. and de Jong, P. J., eds., 15–38, Cambridge University Press, Cambridge (2012).

- [39] Trumpp, A., Rasche, S., Wedekind, D., Rudolf, M., Malberg, H., Matschke, K., and Zaunseder, S., "Relation between pulse pressure and the pulsation strength in camera-based photoplethysmograms," *Curr. Dir. Biomed. Eng.* **3**(2), 489–492 (2017).
- [40] Mourot, L., Bouhaddi, M., and Regnard, J., "Effects of the cold pressor test on cardiac autonomic control in normal subjects.," *Physiol. Res.* **58**, 83–91 (2009).
- [41] Lee, K.-Z., Hung, P.-C., and Tsai, L.-W., "Contact-Free Heart Rate Measurement Using a Camera," in *[2012 Ninth Conf. Comput. Robot Vis.]*, 147–152, IEEE (2012).
- [42] Feng, L., Po, L.-M., Xu, X., Li, Y., Cheung, C.-H., Cheung, K.-W., and Yuan, F., "Dynamic ROI based on K-means for remote photoplethysmography," in *[2015 IEEE Int. Conf. Acoust. Speech Signal Process.]*, **2015-Augus**, 1310–1314, IEEE (2015).
- [43] Wedekind, D., Trumpp, A., Gaetjen, F., Rasche, S., Matschke, K., Malberg, H., and Zaunseder, S., "Assessment of blind source separation techniques for video-based cardiac pulse extraction," *J. Biomed. Opt.* **22**(3), 035002 (2017).